Investigating the effect of a Tumour Necrosis Factor-Alpha (TNF-α) Receptor 2 agonist on 3xTG-Alzheimer mice

Ilse Zwiers (s4535200)

Research project 1 Biomedical Sciences (WMBM901-40)

Research group: Eisel lab (GELIFES)

Supervisor: Irem Bayraktaroglu (Daily), Ulrich Eisel

December 2024-July 2025

Abstract

Alzheimer's disease (AD) is marked by amyloid-beta (Aβ) plaques and tau tangles, with growing evidence linking neuroinflammation to its progression. Tumour Necrosis Factor-alpha (TNF-α) plays a key role in this inflammation. Still, total TNF-α inhibition can cause harmful side effects due to its dual receptor activity: TNFR1 promotes inflammation and cell death, while TNFR2 supports cell survival and reduces inflammation. Targeting these receptors selectively may offer safer treatment options. This study explores the effects of selective TNFR2 activation in wild-type and 3xTG mouse models of AD.

This was investigated by injecting the mice with a TNFR2 agonist either 6 weeks or 12 weeks. After injections, behavioural tests and immunohistochemistry were performed to assess the effects of this agonist.

The results show that the agonist does not alter astrocyte or microglial activation in WT mice, nor does it affect cognition in these animals. There is a tendency toward improved hippocampal memory in agonist-treated female 3xTG mice. In addition, male mice performed better than female mice in the Morris water maze, indicating sex differences in cognition. Although extracellular plaque load was not significantly reduced in agonist-treated mice, intracellular Aβ staining was decreased in agonist-treated male mice. Lastly, working memory was not affected by the treatment compared to controls.

This study shows promising results for using a TNFR2 agonist as a treatment strategy for AD; however, more research is needed to understand the heterogeneity of the human disease.

Table of contents

1. Introduction

1.1 Alzheimer's disease

In 2020, about 1 billion people were over 60, and the World Health Organisation (WHO) expects this to double by 2050. The population over 80 is expected to rise to 426 million in the same time frame, indicating the need to treat age-related diseases (Steverson, 2024). An example of such a disease is Alzheimer's disease (AD), the most prevalent type of dementia worldwide. A cohort study by Kukull et al. (2002) found that the incidence of AD increases significantly with age, rising from 2.8 cases per 1,000 people aged 65–69 to 56.1 cases per 1,000 people over the age of 90. Another study conducted in Rotterdam showed that the prevalence of people with dementia increases over time, with one-third of the population over 85 having AD. Additionally, this study also showed that 75% of all dementia is due to AD (Ott et al., 1995).

1.2 AD pathology

AD is a neurodegenerative disease which is characterised by the formation of amyloid-beta (Aβ) plaques and neurofibrillary tangles (NFTs) in the brain (Tanzi & Bertram, 2005).

According to the widely accepted amyloid hypothesis, the buildup of Aβ causes neuronal death and disease. It has been shown that mutations in the APP gene can cause AD (Sheppard & Coleman, 2020). Aβ plaques form when the transmembrane amyloid precursor protein (APP) is cleaved into several peptides, which can oligomerise and accumulate due to either overproduction or impaired clearance (Breijyeh & Karaman, 2020). These plaques interact with the membrane of cells, compromising their integrity and permeability, ultimately leading to cell death (Bode et al., 2019). Furthermore, these oligomers affect the synaptic density and plasticity. The oligomers increase the glutamate release, an excitatory neurotransmitter in the central nervous system, important for learning. The reduced uptake of glutamate ultimately causes synaptic loss (Shankar et al., 2008).

NFTs are composed of hyperphosphorylated tau protein, which detaches from microtubules and aggregates into filaments that accumulate in axons and dendrites. This leads to the loss of microtubules and other tubulin-associated proteins. The resulting accumulation causes neuronal loss and, consequently, cognitive deficits (Breijyeh & Karaman, 2020).

NFTs are composed of hyperphosphorylated tau protein, which detaches from microtubules and aggregates into filaments that accumulate in axons and dendrites. This leads to the loss of microtubules and other tubulin-associated proteins. The resulting accumulation causes neuronal loss and, consequently, cognitive deficits (Gamblin et al., 2003).

This typical AD pathology is also visible in Figure 1, in which the normal brain is seen in Figure 1A, and an AD brain in Figure 1B.

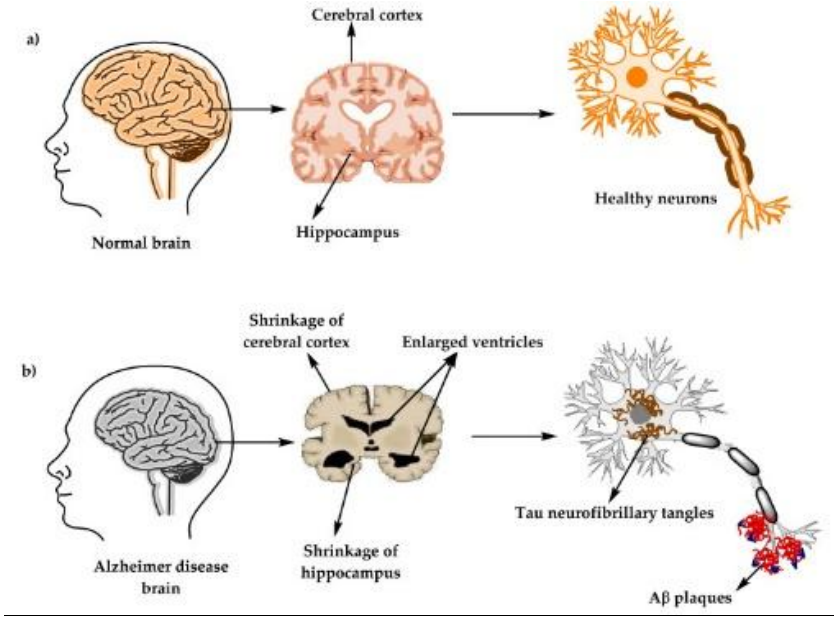

Figure 1: Alzheimer's disease pathology. *The figure shows the differences between a healthy brain (Figure 1A) and an Alzheimer's disease brain (Figure 1B)(Breijyeh & Karaman, 2020).*

1.3 Neuroinflammation

In addition to the amyloid hypothesis explained above, another increasingly researched theory is the inflammation hypothesis. It has been proposed that the accumulation of Aβ can act as a damage-associated molecular pattern (DAMP), activating toll-like receptors (TLRs). This binding activates innate immune cells in the brain, including microglia and astrocytes, which release various cytokines and chemokines (Zhang et al., 2023;DiSabato et al., 2016). Activated microglia and astrocytes can phagocytose Aβ; however, when this process is impaired, it can lead to chronic inflammation and the release of additional pro-inflammatory cytokines and reactive oxygen species (ROS), ultimately resulting in neurotoxicity and degeneration (Walter et al., 2007). Figure 2 shows both the neuroprotective and neurotoxic abilities of microglia. The left side shows normal debris clearance, while the right shows the neurotoxic pathway, where the microglia become pro-inflammatory and cause cell death, due to the impaired clearance of Aβ oligomers.

Several studies have shown that neuroinflammation contributes to cognitive decline. For instance, Lee et al. (2008) used lipopolysaccharides (LPS) to induce inflammation and examine their effect on Aβ accumulation. Their results showed that inflammation increased Aβ accumulation in the hippocampus and caused memory impairment in mice. Another study by Hickman et al. (2008) investigated gene expression in isolated microglia from mice of different ages. They demonstrated that increased cytokine production impairs Aβ clearance and, over time, downregulates genes involved in this process, further promoting Aβ accumulation. In addition to microglia, astrocytes also play a significant role in neuroinflammation and Alzheimer's disease (Wyss-Coray et al., 2003). Astrocytes help bind and clear Aβ; however, their impaired function contributes to reduced Aβ clearance and disease progression.

Neuroinflammation, driven by glial cell activation and the release of pro-inflammatory cytokines, is now recognised as a key contributor to AD progression. One major cytokine released during this process is tumour necrosis factor-alpha (TNF-α), which plays a central role in mediating inflammatory responses and neuronal dysfunction(Idriss & Naismith, 2000).

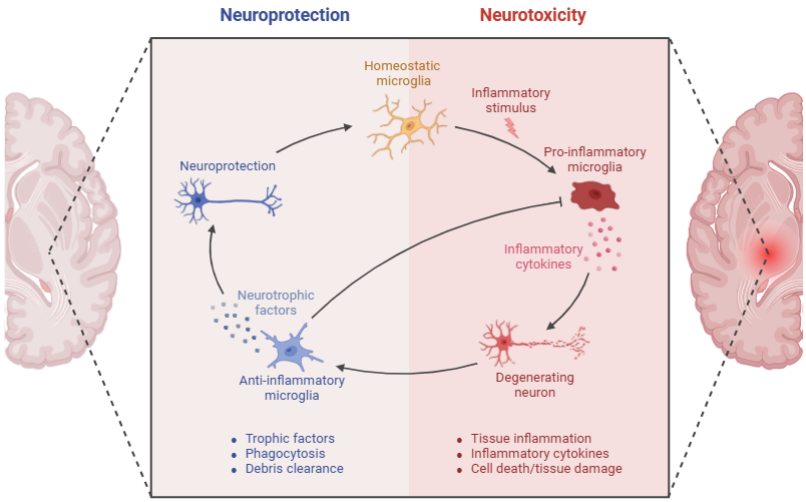

Figure 2: Active versus chronic inflammation in AD. *This Figure shows both the neuroprotective and neurotoxic abilities of microglia and inflammation. The left part of the figure shows the neuroprotective capacities, which clears debris, and the right part of the figure shows the chronic inflammation and therefore tissue damage and cell death (Biorender).*

1.4 TNF-α

Tumour Necrosis Factor Alpha (TNF-α) is an inflammatory cytokine produced by macrophages, monocytes, and microglia during acute inflammation. It is responsible for a diverse range of intracellular signalling events that can lead to necrosis or apoptosis (Idriss & Naismith, 2000). TNF-α is a type II transmembrane protein that exists in two forms: a membrane-bound form (mTNF), which can be cleaved to produce a soluble form (sTNF) (Fischer et al., 2015). TNF-α signals through two distinct receptors: TNF receptor 1 (TNFR1) and TNF receptor 2 (TNFR2). TNFR1 is expressed in nearly all cell types, whereas TNFR2 expression is more restricted—predominantly found on immune cells (particularly regulatory T cells, or Tregs), as well as on endothelial and neuronal cells (Dong et al., 2015). Notably, TNFR2 has been shown to promote Treg expansion and function, as demonstrated in a study on graft-versus-host disease (Chopra et al., 2016). While TNFR1 is activated by both mTNF and sTNF, TNFR2 is activated exclusively by sTNF. The two receptors have markedly different functions: TNFR1 is associated with neurodegeneration, whereas TNFR2 is linked to neuroprotection (Dong et al., 2015).

1.5 TNF receptor 1 and TNF receptor 2

TNFR1 contains a cytoplasmic death domain, enabling it to initiate divergent intracellular signalling pathways upon activation. When TNF binds to TNFR1, TRADD (TNFR1-associated death domain protein) is recruited. This leads either to the activation of the transcription factor NF-κB, promoting cell survival, or to the engagement of cell death pathways such as apoptosis and necroptosis. Figure 3A illustrates the different signalling complexes activated by TNFR1 (Dong et al., 2015).

TNFR2, by contrast, lacks a death domain and activates pathways involved in cell survival and regeneration (Figure 3B). Binding to TNFR2 leads to the activation of TRAF1/2 and other downstream molecules; however, the full scope of these pathways remains less well understood.

TRAF2 is a key mediator in this signalling cascade, triggering the downstream activation of NF-κB and thereby promoting cell survival (Dong et al., 2016).

Studies using TNF-α-deficient mice, which exhibit increased susceptibility to infections, highlight the essential role of TNF-α in immune defense(Fischer et al., 2015).

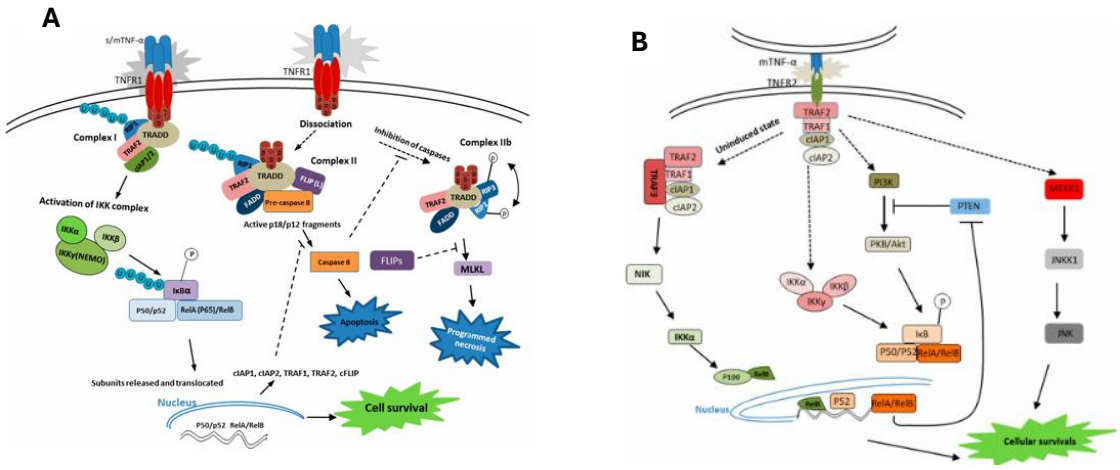

Figure 3: Signalling pathways of TNF receptor 1 and 2. *A) Signalling pathways of TNFR1. B) Signalling pathways of TNFR2 (Dong et al., 2015).*

1.6 The connection between neuroinflammation and AD

The chronic inflammatory state contributes to progressive neuronal damage, as seen in neurodegenerative conditions such as AD (Fischer & Maier, 2015). This proposes a possible connection between chronic inflammation caused by TNF-α and the progression of AD. This connection has been studied a lot, and it has been shown that neuroinflammation is associated with neurodegeneration and the progression of disease pathology. The role of TNF in AD has been described in multiple papers. For example a meta-analysis by Bona et al. (2009), examined the association between TNF-α polymorphisms and the risk of AD. This analysis showed that several polymorphisms can cause a higher risk for developing AD, and supports the hypothesis that TNF-α is involved in the progression of AD.

Levels of inflammatory cytokines such as IL-1, IL-6, and TNF-α are elevated in AD patients compared to healthy controls, and even vary between AD patients at different stages of the disease (Tansey & McAlpine, 2008). In a study by Kitazawa et al. (2008), the effect of LPS-induced inflammation was investigated in triple transgenic (3xTG) mice by measuring microglial activation, plaque formation, and tangle development. The results showed that microglial activation exacerbates AD pathology in these mice.

Similarly, a study by Fillit et al. (1991), measured TNF-α levels in both AD patients and healthy controls, finding that TNF-α levels were significantly higher in the AD group, further supporting its involvement in neurodegeneration.

Another support to the connection between TNF- α and AD progression is the fact that microglia are more activated during AD, and it has been shown that TNF-α levels are increased in these microglia associated with Aβ plaques (Koenigsknecht-Talboo & Landreth, 2005).

Given the high prevalence of AD among the elderly and the burden it places on caregivers and healthcare systems, it is crucial to develop effective treatment strategies. Currently, available treatments are symptomatic, targeting neurotransmitter imbalances or reducing plaque and tangle formation. These drugs include donepezil, galantamine, rivastigmine, and memantine (Yiannopoulou & Papageorgiou, 2020).

The evidence linking TNF-α to AD pathogenesis suggests it may serve as a disease-modifying therapeutic target. One potential approach is the complete blockade of TNF-α. Several anti-TNF agents, such as etanercept, adalimumab, and infliximab, are already used for inflammatory diseases like rheumatoid arthritis (Torres-Acosta et al., 2020). Examples are Etanercept, adalimumab and infliximab (Torres-Acosta et al., 2020). Adalimumab and infliximab are monoclonal antibodies that bind to TNF-α, while etanercept is a dimeric fusion protein that binds and inactivates TNF (Torres-Acosta et al., 2020). There have been several studies that have studied the effect of blocking TNF in AD; however, this blocking has resulted in severe side effects, including an increased risk for infection (Li et al., 2021). A meta-analysis by Singh et al. (2011) reported that TNF inhibitors increase the risk of side effects such as serious infections and induction of autoantibodies.

These side effects may be explained by the distinct roles of the TNF receptors: TNFR1 is pro-inflammatory and neurodegenerative, whereas TNFR2 is neuroprotective. Thus, instead of global TNF-α blockade, a more refined approach may involve selective inhibition of TNFR1 or activation of TNFR2.

This selective activation or repression of either receptor has been studied in various studies. For example, Ortí-Casañ, Boerema, et al. (2023), studied the effect of a TNFR1 antagonist Atrosimab, in an acute mouse model for AD. This acute model used an NMDA-induced lesion that mimics neurodegenerative disease symptoms. The study showed that Atrosimab is effective in ameliorating disease functions in this model. There was an improvement in cognitive function and reduced neuroinflammation and neuronal cell death. Similarly, Richter et al. (2019) used a monovalent anti-TNF antibody fragment to inhibit TNFR1. This study showed that Atrosimab potently inhibits TNF-induced activation of TNFR1. Next to inhibition of TNFR1, the activation of TNFR2 has also been studied, showing that the administration of a TNFR2 agonist either centrally or through intraperitoneal injections in J20 mice. This administration reduced the Aβ deposits and BACE 1 levels. Next to this, the microglial and astrocytic activation was also improved after treatment (Ortí-Casañ et al., 2022). Another study by Ortí-Casañ, Wajant, et al. (2023), which also studied the effect of a TNFR2 agonist on J20/huTNFR2 mice, showed the same results and also showed an improvement of cognitive function in AD mice. These mice have a humanised TNFR2 domain, which makes the model only respond to human compounds.

1.7 Mouse models

To study the activation or repression of the receptors, suitable in vivo models are needed, which can mimic the pathological and behavioural features of Alzheimer's disease. Mouse models are very valuable for this, as these models can be manipulated in a controlled environment and are easy to monitor for longer periods of time. There are many different mouse models for Alzheimer's

disease, examples being APP23 and 3xTG mice models. These mouse models have different genetic backgrounds, disease onset times and progression.

The B6;129-Tg (APPSwe, tauP301L)1Lfa Psen1^{tm1Mpm}/Mmjax (3xTG) mouse model harbours three mutations associated with familial AD: enabling it to develop both Aβ plaques and neurofibrillary tangles. This dual pathology provides a valuable model for studying the interplay between amyloid and tau pathologies. Aβ deposition begins at approximately 3 months of age, while tau pathology typically becomes apparent between 10 to 12 months (Oddo et al., 2003). Another advantage of the 3xTG model is the early onset of cognitive decline, observable between 3–5 months, with behavioural changes detectable as early as 2.5 months (Roda et al., 2020). These features make the 3xTG mouse particularly suitable for evaluating both behavioural outcomes and neurodegenerative progression.

Further supporting the utility of the 3xTG model is its ability to replicate the synergistic relationship between Aβ and tau pathology. As noted earlier, these pathologies influence each other. A study by Chabrier et al. (2014), which examined the combined effects of Aβ and human tau in a double transgenic mouse model, showed that Aβ-dependent increases in tau pathology significantly contributed to dendritic spine alterations and cognitive impairment. (Chabrier et al., 2014). This makes the 3xTG mouse model very suitable for mimicking the normal progression of the disease.

In contrast, the wild-type (WT) C57BL/6J mouse line serves as a healthy control. This strain does not carry any AD-associated mutations and represents normal ageing. It is often used to study the effects of treatments in non-diseased animals, allowing researchers to assess potential side effects or off-target effects of interventions. WT mice do not exhibit cognitive deficits or AD-like neuropathology (Javonillo et al., 2022; Samaey et al., 2019)

1.8 Research question and hypothesis

The research question that is going to be answered in this report is “What is the effect of selective activation of TNFR2 in 3xTG and WT mouse models?”. To answer this main question, 2 sub-questions are going to help with this, namely (1)” What is the effect of this selective activation in terms of cognitive abilities?” and (2)” What is the effect of the modulation of TNFR2 on brain pathology in these mice?” Based on the information mentioned above, it is expected that there will be several effects of the agonist on these 2 mouse models.

Firstly, after treatment with the WT mice, there will be no difference in pathology or behaviour within the treated or control group. This is expected because in these mice there is no increased neurodegeneration, and therefore the agonist does not increase cell survival more in the treatment group compared to the PBS group.

Secondly, in the 3xTG mice, it is expected that there will be fewer cognitive deficits seen in the mice treated with the agonist, compared to the PBS-treated mice. For the pathology in the brains of these mice, it is expected that both the amyloid and Tau burden will be decreased in the treated animals compared to controls, because the agonist will decrease the amount of inflammation, and therefore increase the amyloid clearance of microglia.

To test this hypothesis, the mice will be injected with either the compound or PBS for 6/12 weeks. Behavioural tests such as an Elevated Plus Maze (EPM), Y-maze and Morris Water Maze (MWM) will be performed to assess cognition. After behavioural tests, the brains will be analysed using immunohistochemistry, visualising plaque, tangle formation and inflammation. The peripheral effects of the treatment will be tested in the blood using FACS.

2. Methods

2.1 Mice

Mice were bred at University of Groningen. The WT mice have a C57BL/6J background. The 3xTG mice have a B6;129 background, are homozygous for the Psen1^{tm1Mpm} mutation, and are homozygous for the co-injected APPSwe and tauP301L transgenes.

Mice got food and water available ad libitum and were on a 12:12 h light/dark cycle. All procedures were carried out according to regulations and guidelines related to animal research.

2.2 Treatment

Mice were injected with either the compound or phosphate-buffered saline (PBS) (#10010031**,** Gibco) 2 times per week via intraperitoneal injection. The treatment groups of the 3xTG mice are shown in Table 1, and the groups of the WT mice in Table 2.

Table 1: Treatment groups of the TNFR2 agonist experiment with 3xTG AD mice. *The table shows the groups, the number of animals per group and the treatment each group received.*

Groups	**Number of animals**	**Treatment**
3xTG Male group	12	150 µl of agonist (**10mg/ml)**
3xTG Male control group	12	150 µl of PBS
3xTG Female group	15	150 µl of agonist (**10mg/ml)**
3xTG Female control group	15	150 µl of PBS

Table 2: Treatment groups of the TNFR2 agonist experiment with WT mice. *The table shows the groups, the number of animals per group and the treatment each group received.*

Groups	**Number of animals**	**Treatment**
WT Male experimental group	11	150 µl of agonist
WT Male control group	11	150 µl of PBS

2.3 Behavioural tests

Before starting the behavioural tests, the mice were habituated for 5 days to get used to handling and the experimental rooms. Habituation was done by placing the mouse on the researcher's hand for 2 minutes in each of the experimental rooms. Each mouse was handled separately.

2.3.1 Elevated plus maze

The elevated plus maze was used to assess anxiety levels. This test counts how many times a mouse goes onto the open arms of the maze. The maze has 2 open arms (5.5 cm wide x 30 cm long) and 2 closed arms (5.5 cm wide x 30 cm long x 15 cm high) opposite from each other, making a plus shape. The light intensity was 10 lx in the centre of the maze, and 12 lx in the open arms. The mouse is placed in the maze for 8 minutes and can explore freely. During the exploration, the number of entries in each arm, total entries, distance moved, as well as the percentage of time spent in the centre, open and closed arms were recorded and scored using the EthoVision 11.5 software (Noldus).

2.3.2 Y-maze

Next, a Y-maze was performed to assess the working memory of the mice. The Y-maze had 3 arms (40 cm long x 8 cm wide) separated from each other at an angle of 120°. The light intensity was set to 10 lx. The mouse is placed in the middle of the maze and can roam freely for 10 minutes. The number of entries in the different arms of the maze is recorded in the order of entry, and it is an entry when all 4 legs have entered the arm. The alternating percentages are calculated by summing up the total amount of triads made, divided by the total number of entries made minus two. A triad is three consecutive entries in the 3 different arms.

2.3.3 Morris water maze (MWM)

Lastly, to measure the hippocampal memory of the mice, an MWM was performed. The pool had a diameter of 135 cm, and a constant water temperature of 24 degrees was maintained. Water-based, non-toxic white paint (Flexa Powerdek) was added to the water to make the platform invisible for the mice. The platform (15 cm diameter) was placed 1.5-2 cm under the water surface. Visual cues are placed on the walls around the room, and the light intensity was 40 lx at the centre of the pool.

This test lasts ten days, of which the first 8 days will be training days, during which the mice will learn where the platform is. Each mouse has 4 trials each day, in which the mouse is placed in the pool in different places, the mouse has 120 seconds to find the platform, and after finding the platform has to sit on this platform for 20 seconds before being picked up and put back in the cage. In the case that the mouse cannot find the platform, the mouse is guided to the platform and also has to sit on this platform for 20 seconds before being removed from the pool. This ensures that the mice can find the platform. After training, there are 2 probe trials, in which the platform has been removed to assess the memory. During these probe trials, the mice could explore the pool freely.

This exploration was recorded with EthoVision 11.5 software, and several parameters were stored. These parameters include the time spent in each quadrant, time spent in the target quadrant, the number of times the mice crossed the platform, latency to platform, velocity, and the distance that the mice swam.

The results were analysed in both the controls and compound-treated groups and compared with each other.

2.4 Sacrifice, perfusion and tissue preparation

Animals were anesthetised with 0.1-0.3 mL of pentobarbital (Euthasol, 20%, Dechra), and blood was collected for further analysis via a heart puncture in the left ventricle. The animal was first rinsed with a rinsing solution (0.9% NaCl + Heparin), after which the animal is fixed with 100 mL 4% PFA. After perfusion, both the brain and spleen were collected in cups containing 4% PFA to use for later analysis. The brains were left in the PFA for 24 hours for post-fixation, after which they were washed with PB (0.01M) 6 times every half hour. The cups stayed on a shaker at 100 rpm at room temperature (RT).

After washing, the brains were put in a 30% sucrose solution to protect against damage during freezing. The brains stay in the solution for 24h, and sucrose is refreshed after 24h when the brains have not sunk to the bottom of the cup. After all brains had sunk, the brains and spleens were frozen with liquid nitrogen and stored at -20 degrees. Brains were cut at -20°C in slices of 20 µm–

thick coronal sections using a cryostat (Slee MNT). Slices were stored at 4°C in PBSA (until further use.

2.5 Immunohistochemistry with 6e10, CD68, IBA-1, GFAP

The cut brain sections were selected for staining and washed with Tris-buffered saline (TBS) (0.01 M, pH 7.4). Next, sections were blocked in TBS containing 0.3% TritonX-100 (Thermo Scientific) and 3% Bovine Albumin Serum (BSA) (#1003618249, Sigma-Aldrich) at room temperature for one hour. After blocking, slices were incubated with a primary antibody (Table 3) in TBS containing 0.3% TritonX and 3% BSA overnight at 4°C. After primary antibody incubation and thorough washing with TBS, cells were incubated with corresponding Alexa Fluor-conjugated secondary antibodies (Table 4) in TBS containing 0.3% TritonX and 3% BSA at room temperature for 2 hours. The slices were washed and mounted using Vectashield (H-1800-10, VectorLab) to prevent fading of the fluorescent staining. The staining was visualised using the Leica DMI6000 B microscope (Leica Microsystems).

Table 3: Primary antibodies used during immunohistochemistry. *This table shows the Primary antibodies that were used during experiments. The table shows the type of antibody, the dilution of the antibody, the product number and the company.*

Antibody	Dilution	Product number	Company
mouse anti 6e10	1:2000	#803003	Biolegend
mouse anti-GFAP	1:10000	#G3893	Sigma
rabbit anti-Iba1	1:2500	#019–19741	Wako Chemicals
rat anti-CD68	1:1000	#MCA1957GA	Biorad

Table 4: Secondary antibodies used during immunohistochemistry. *This table shows the secondary antibodies that were used during experiments. The table shows the type of antibody, the antibody dilution, the product number and the company.*

Antibody	Dilution	Product number	Company
Donkey anti-rabbit 647	1:500	A31573	Invitrogen
Donkey anti-mouse 555	1:500	A31570	Invitrogen
Donkey anti-rat 488	1:500	A21208	Invitrogen

2.6 DAB immunohistochemistry with AT8

Tissue sections were washed in 0.01 M Tris-buffered saline (TBS; 3 × 5 min), then incubated in 0.3% hydrogen peroxide (1.07209, Merck) for 30 minutes to quench endogenous peroxidase activity, followed by another TBS wash (3 × 5 min). Sections were then incubated with primary antibody (mouse anti-AT8, Invitrogen, 1:1000) in 0.01 M TBS containing 1% BSA and 0.5% Triton X-100 for 2 hours at room temperature on a shaker, and subsequently for about 72 hours at 4°C.
After washing (4 × 5 min, TBS), sections were incubated with a biotinylated goat anti-mouse secondary antibody (1:500, Jackson ImmunoResearch, 115-065-166) for 2 hours, followed by another TBS wash (4 × 5 min). Sections were then incubated in avidin-biotin complex (ABC; 1:500 in TBS, prepared 30 minutes in advance) for 2 hours and washed again (4 × 5 min).
For visualisation, DAB tablets were dissolved in Milli-Q water (3 mL) and stirred for ≥10 minutes. The DAB solution was activated with 0.01% H_2O_2 and applied for 16 minutes and 10 seconds, followed by 3 quick washes and final washes (3 × 5 min, TBS). Sections were mounted in 1% gelatine and dried overnight.

Dehydration was performed through a graded ethanol and xylene series (100% ethanol ×2, 70% EtOH/30% xylene, 30% EtOH/70% xylene, 100% xylene ×3; 5 min each). Slides were cover slipped with DPX (#06522, Sigma-Aldrich) and left to dry for 1–2 nights.

2.7 FACS analysis of the blood

Whole blood samples were centrifuged at 460xg for 6 minutes, and the supernatant (serum) was carefully removed and stored at -20°C. Three unstained control tubes were processed alongside the stained samples. The remaining pellets were stained extracellularly with a primary antibody mix (Appendix A1), according to the protocol provided by BioNTech. The staining was fixed and permeabilised with a Fix/Perm solution (1:3, #00-5223-56, Invitrogen) and washed with Perm buffer (#00-5123-43, Invitrogen). After permeabilisation, the blood was incubated with a secondary antibody mix (FoxP3, 1:100, #25-5773-82, Invitrogen) to stain the blood intracellularly. After incubation and washing with Perm buffer, the cells were stored in 100 mL FACS buffer (DPBS + BSA + 1mM EDTA) at 4 °C, before sending to BioNTech for further analysis (Mainz, Germany).

2.8 Analysis

Brain slices were analysed using Fiji ImageJ, in which different Regions of interest (ROI) were selected (Appendix A2 and A3). A percentage of coverage was determined after setting a certain threshold based on visual observation. After quantification, the results were visualised, and statistical analyses were conducted using GraphPad Prism 8.0.

2.9 Statistics

Results were analysed with an unpaired Student's t test when comparing two normally distributed groups or a Mann-Whitney test when data were not normally distributed. Normality was assessed using the Shapiro-Wilk test. A Two-way ANOVA followed by Sidak's multiple-comparison test were used to analyse multiple groups. All statistical tests performed were two-tailed. All data are reported as mean ± SEM, and statistically significant differences were considered when $p < 0,05$.

3. Results

3.1 Treatment with the TNFR2 agonist does not change cognition in WT mice compared to controls

To assess working memory in WT mice, a Y-maze was performed. Figure 4 shows the results of the y-maze. The x-axis shows the experimental groups: Male PBS (Grey, n=11) and Male TNFR2 agonist (Green, n=11). The y-axis shows the alternation in percentages. This graph shows that there is no difference in alternation between the groups; both groups have an alternation of about 50-60%.

To evaluate hippocampal memory, an MWM was performed. Figures 5 and 6 show the results of both the training period (Figure 5) and the probe trial (Figure 6). In Figure 5, it is visible that there is no difference in escape latency between the groups over all 8 training days, which are displayed on the x-axis. The escape latency does decrease over time. Figure 6 shows no difference between the groups during the probe trials. In Graph 6A, both groups crossed the platform location about five times. Similarly, graph 6B shows that both groups spent approximately 40% of the time in the target quadrant.

Based on these results, no significant differences were observed between Male PBS- and Male TNFR2 agonist-treated mice in measures of working memory or hippocampal-dependent spatial memory, indicating that TNFR2 agonist treatment did not affect cognitive performance in these behavioural tasks.

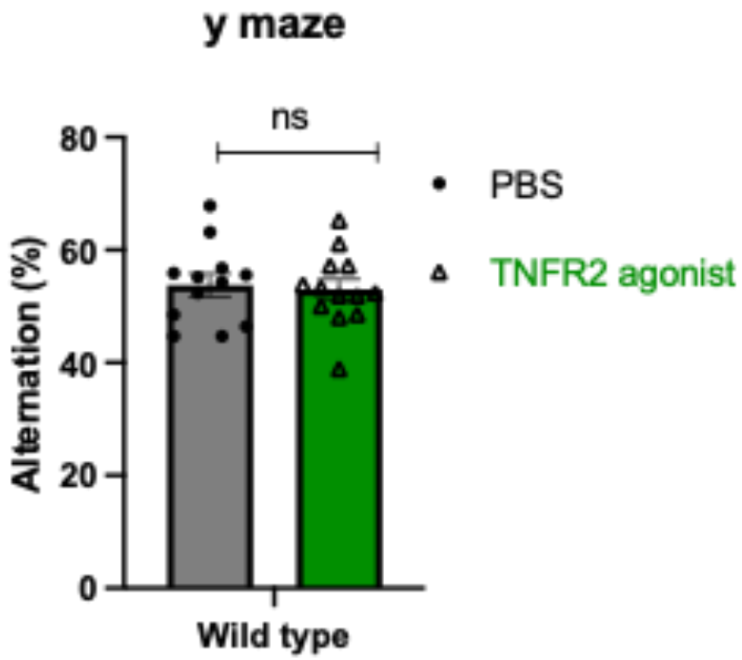

Figure 4: Treatment with the TNFR2 agonist does not affect working memory in WT mice. *The x-axis shows the different groups: Male PBS (Grey) (n=11), Male Compound (Green) (n=11), and the Y-axis shows the alternation in percentages (Alternation (%)). Data represented as mean ± SEM. *p<0.05, **p<0.01.*

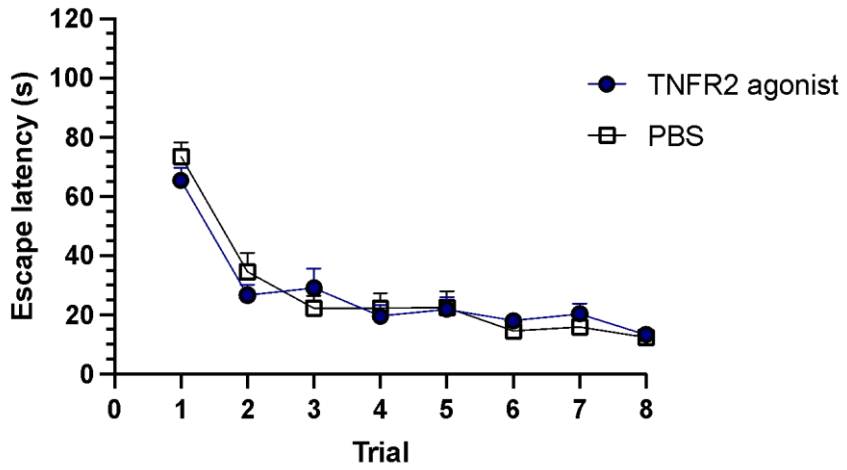

Figure 5: TNFR2 treatment does not affect hippocampal memory during MWM training in WT mice. *This figure shows the results of the probe trial of the MWM. The x-axis shows the trial days (Trial). There are two groups: Male PBS (White square) (n=11), Male Compound (Blue circle) (n=11). The y-axis shows the escape latency in seconds (Escape latency (s)). Data represented as mean ± SEM. *p<0.05, **p<0.01.*

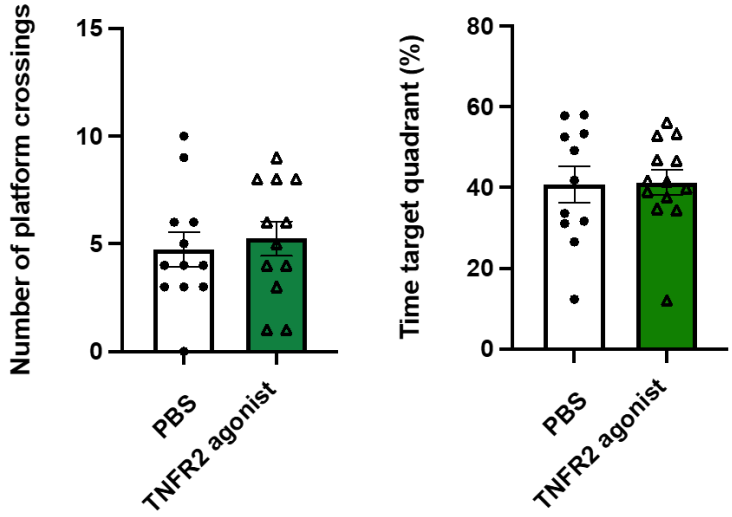

Figure 6: TNFR2 treatment does not affect hippocampal memory during the MWM probe trial in WT mice. *This figure shows the results of the probe trial of the MWM. The x-axis shows the different groups: Male PBS (Grey) (n=11), Male Compound (Green) (n=11). Figure 6A shows the number of times the platform was crossed (Number of platform crossings). Figure 6B shows the time the mice spent in the target quadrant in percentages (Time target quadrant (%)). Data represented as mean ± SEM. *p<0.05, **p<0.01.*

3.2 GFAP and CD68 staining show no significant differences between treated and control WT mice

To investigate the effects of the TNFR2 agonist (Compound) in healthy wild-type mice, these mice were injected with the compound or PBS for 6 weeks. Both groups consisted of 11 male mice each. After injections, the mice were subjected to behavioural tests and were sacrificed for further analysis. The staining results of both the GFAP and CD68 staining are visible in Figure A4. Figure 7 shows the quantified results of GFAP staining in 4 regions of the brain. Staining with GFAP

visualises the astrocytes that are present in the brain. Graph 7A shows that there are no significant results between PBS-treated mice and compound-treated mice in the CA1 region of the hippocampus. This result is also seen in both the CA3 region and the dentate gyrus of the hippocampus (Figure 7B, 7C). In Figure 7D, the quantification of the corpus callosum is visible. This shows that there is no statistical difference between the 2 groups, as the p-value is 1.000.

Figure 8 shows the quantified results of a CD68 staining in 3 brain regions. CD68 shows the phagocytic microglia present in the brain. In all three regions of the brain that have been measured, which are the hippocampus, corpus callosum and cortex (Figure 8A, B, C), there is no difference between treatment groups visible.

These findings indicate that the compound does not induce neuroinflammation under non-pathological conditions.

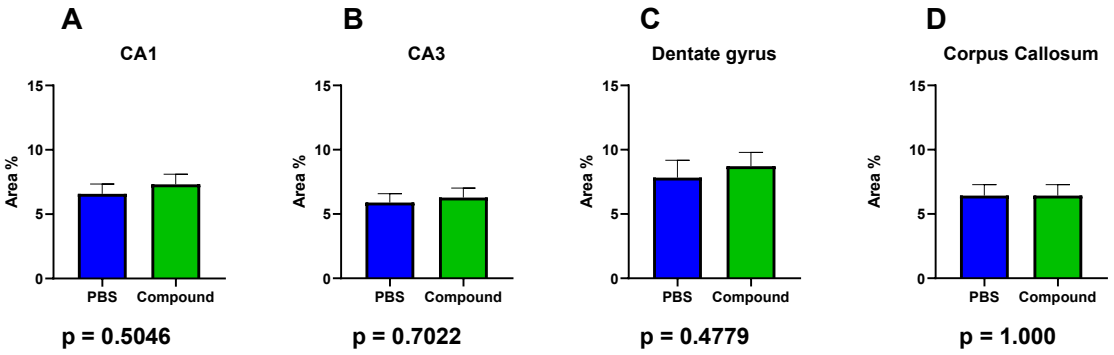

Figure 7: No significant differences between treated and control groups are visible in GFAP staining in WT mice. *The figure shows the results of the GFAP staining in WT mice. The x-axis shows the 2 different groups (PBS (n=11) and Compound (n=11)), while the y-axis shows the percentage of GFAP visible in the brain regions. A) shows the quantification of the GFAP staining in the CA1 region of the hippocampus, and B) quantification of the GFAP staining in the CA3 region of the hippocampus. C) Quantification of the GFAP staining in the dentate gyrus (DG). D) Quantification of the GFAP staining in the corpus callosum. Below each graph, the p-value has been displayed. Data represented as mean ± SEM. *p<0.05, **p<0.01.*

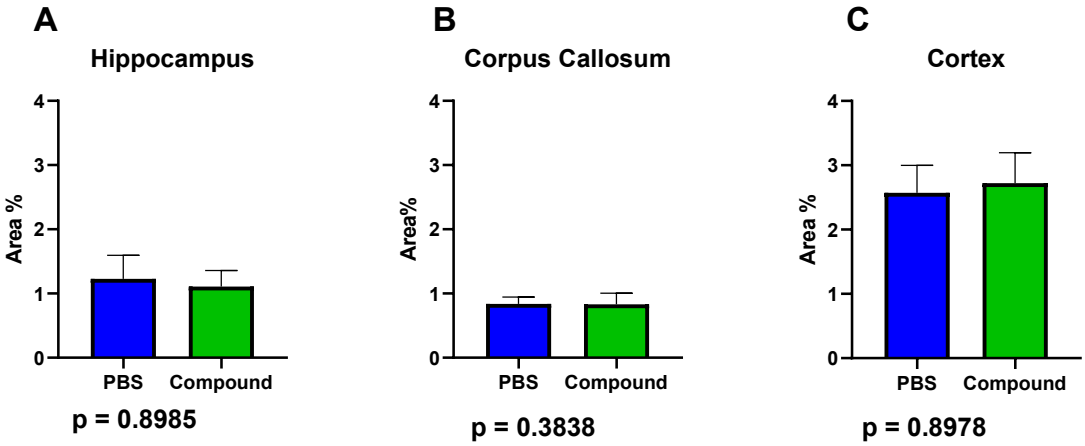

Figure 8: No significant difference is seen between treated and controls after CD68 staining in WT mice. *The figure shows the results of the CD68 staining in WT mice. The x-axis shows the 2 different groups (PBS(n=11) and Compound(n=11)), while the y-axis shows the percentage of CD68 visible in the brain regions. A) shows the quantification of the staining of the whole hippocampus, and B) quantification of the*

*staining in the corpus callosum. C) Quantification of the CD68 staining in the cortex. Under each graph, the corresponding p-value has been displayed. Data represented as mean ± SEM. *p<0.05, **p<0.01.*

3.3 Working memory is not affected in 3xTG mice after treatment with the TNFR2 agonist

To assess working memory in 3xTG mice, a y-maze was performed, and mice with a total number of entries lower than 8 were excluded. Figure 9 shows the results of the y-maze. The x-axis shows the experimental groups: Male PBS (Blue) (n=6), Male Compound (Green) (n=4), Female PBS (Red) (n=12), Female Compound (Purple) (n=11). Figure 9A shows the spontaneous alternation of the mice in percentages. It is visible that there is no difference between the male and female groups. It is visible that the females have a higher percentage compared to males, but this is not significantly different.

Figure 9B shows the total number of entries of the groups. In the males, there is no difference seen between the compound and PBS groups. When looking at the female mice, it is visible that the PBS group has fewer entries compared to the compound group, but no significant differences are observed. When comparing the male mice with the female mice, there is again no significant difference between male and female mice; however, it is visible that the females have a slightly higher number of entries.

This data suggests that there are no significant differences in working memory performance between male and female mice or between treatment groups.

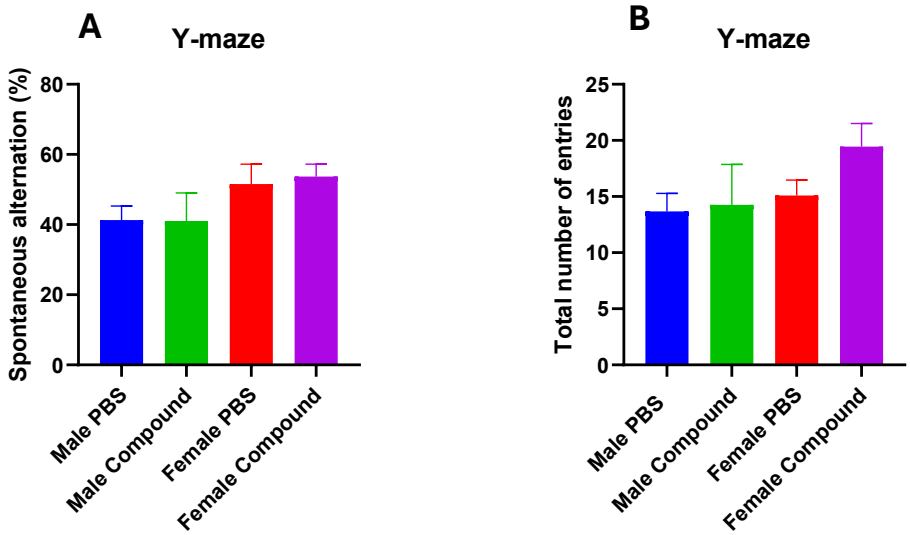

Figure 9: Working memory is not affected in 3xTG mice. *The x-axis shows the different groups: Male PBS (Blue) (n=6), Male Compound (Green) (n=4), Female PBS (Red) (n=12), Female Compound (Purple) (n=11). Figure A shows the spontaneous alternation of the mice on the y-axis (Spontaneous alternation (%)). Figure B shows the Total number of entries of the mice, which is displayed on the y-axis. Data represented as mean ± SEM. *p<0.05, **p<0.01.*

3.4 There is a tendency for improvement in female mice treated with the agonist, compared to controls

To assess the hippocampal memory of the mice, a Morris Water maze was performed, which consisted of 8 training days and 2 probe trials. Figures 10 and 11 show the results of the MWM. The groups are shown as follows: Male PBS (Blue) (n=10), Male Compound (Green) (n=10), Female PBS (Red) (n=14), Female Compound (Purple) (n=15).

Figure 10 shows the results of the training period of 8 days, in which the mice were supposed to learn where the platform was. The graph shows the escape latency in seconds on the y-axis and the days on the x-axis. The different lines represent the different groups. It is visible that the males learn and remember better where the platform is than the females, as the escape latency is lower in these mice. There is a significant difference in escape latency between the PBS-treated females and PBS-treated males, which means that the PBS males learn significantly better than the PBS females. Within the females, it is visible that the compound-treated mice perform better than the PBS-treated mice; however, there is no significant difference seen. Within the males, there is no difference seen; the escape latency of both male groups looks similar.

Figure 11 shows the results of the probe trials. The x-axis of each graph shows the different groups, and the y-axis displays either the time spent in the target quadrant or the platform crossings.

Figure 11A shows the time that the mice spent in the target quadrant of probe trial 1, which shows no differences between groups, with only the male PBS group having a slightly higher time compared to the other groups. Figure 11B shows the time spent in the target quadrant of the second probe trials and shows no significant differences between groups. There is a slight increase in the time of the female compound group visible.

Figure 11C shows the platform crossings of the mice for probe trial 1, and there is a clear trend visible that the male mice have a higher number of crossings compared to females, but no significant differences. Within the male groups, no difference is visible between PBS and compound-treated mice. Between the female PBS and compound-treated mice, it is visible that the compound-treated females have a higher number of crossings compared to PBS-treated mice.

Lastly, Figure 11D shows the platform crossings of the second probe trial and shows that there is a significant difference between the PBS-treated female mice and the PBS-treated male mice, with a p-value of 0.01996. Similar to the first probe trial, the male mice performed better in the second trial compared to the females and had more platform crossings. Between the male mice, it is visible that the compound-treated mice have fewer crossings compared to the PBS-treated mice. The opposite is seen in the female mice, where the PBS-treated mice have fewer crossings than the compound-treated female mice.

This data suggests that male mice exhibit better spatial learning and memory compared to females, with a significant difference observed between PBS-treated males and females. Additionally, the compound may have a tendency of enhancing the memory in female mice.

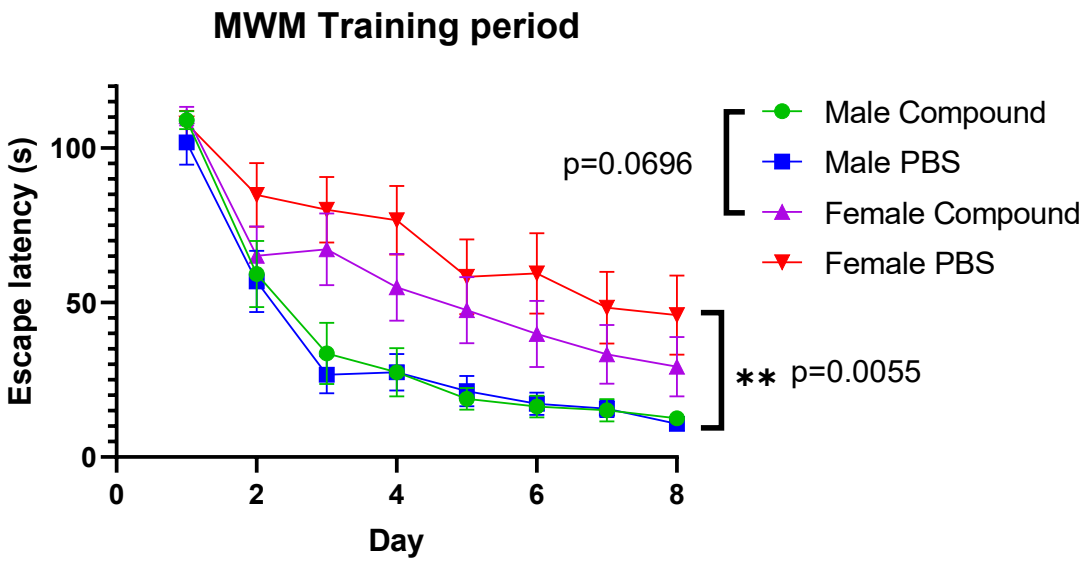

Figure 10: Male mice perform better during the training period compared to female mice. *This graph shows the escape latency (s) of the different experimental groups during the training period of the MWM. The x-axis shows the days of training, and the y-axis shows the escape latency in seconds (Escape latency (s)). The groups are as follows: Male PBS (Blue) (n=10), Male Compound (Green) (n=10), Female PBS (Red) (n=14), Female Compound (Purple) (n=15). Data represented as mean ± SEM. *p<0.05, **p<0.01.*

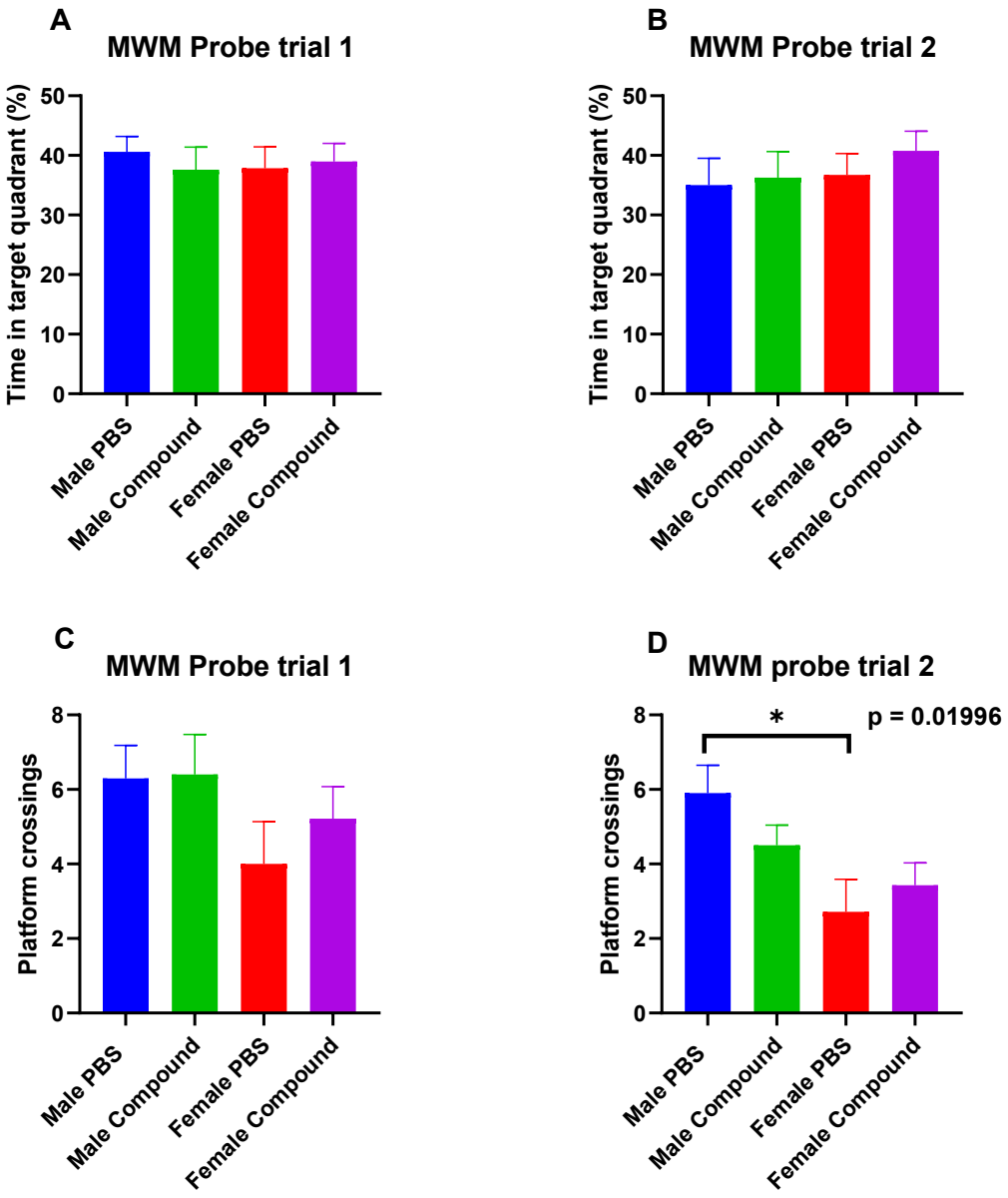

Figure 11: Male PBS mice cross the platform significantly more than female PBS mice during probe trial 2. *This graph shows the results of both probe trials of the MWM. The x-axis shows the different groups: Male PBS (Blue) (n=10), Male Compound (Green) (n=10), Female PBS (Red) (n=14), Female Compound (Purple) (n=15). The y-axis shows either the time spent in the target quadrant (s) or the number of platform crossings. Figure 11A and C show the results of probe trial 1, in which graph A shows the time spent in the target quadrant and graph C shows the number of platform crossings. Figure 11B and D show the results of probe trial 2, in which graph C shows the time spent in the target quadrant and graph D shows the platform crossings. Data represented as mean ± SEM. *p<0.05, **p<0.01.*

3.5 Plaque load is not significantly altered in 3xTG mice after treatment with the agonist, compared to controls

To evaluate the effect of TNFR2 treatment on 3xTG mice, these mice were injected with either the compound or PBS for 12 weeks. After the injections, the mice were subjected to behavioural tests and then killed for further analysis. The brain slices were stained with 6e10 to visualise the Aβ that is present in these brains. This staining is seen in the pictures in Figure 12, where the top picture shows the subiculum of a female mouse treated with the TNFR2 agonist, and the bottom picture shows a female PBS-treated mouse. There were 4 experimental groups: Male PBS (n=6), Male Compound (n=6), Female PBS (n=13), Female Compound (n=13), which were analysed.

Figure 12 shows the result of this quantification in the subiculum of the ventral hippocampus. The x-axis shows the different experimental groups, and the y-axis shows the coverage of staining in percentages (Coverage %). Figure 12A shows the extracellular staining of 6e10 and shows an increase after treatment with the agonist in females; however, this increase is not significant. In males, there were no extracellular plaques seen, which is why there are no results visible. Figure 12B shows the intracellular staining of 6e10 in these brain slices. This shows a decrease in intracellular staining in male mice treated with the agonist compared to PBS-treated males. There is a slight decrease in agonist-treated females compared to PBS-treated females, but in both sexes this difference was not significant.

This data suggests that TNFR2 agonist treatment may reduce intracellular Aβ accumulation in males, while having no significant effect on extracellular Aβ in females.

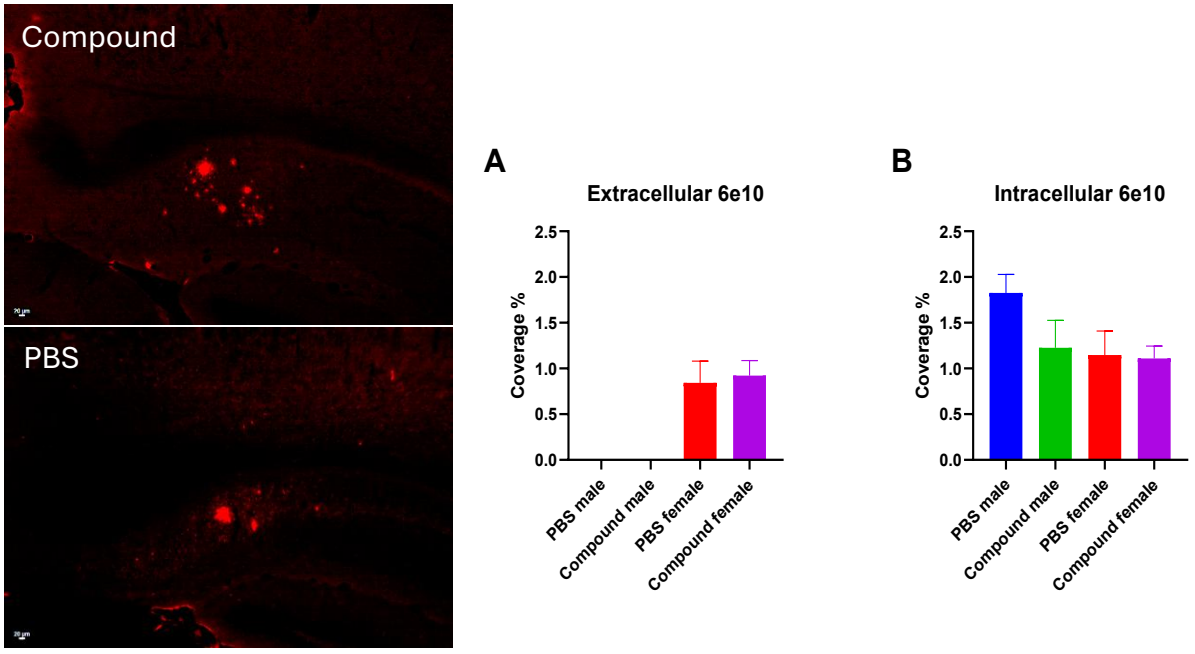

Figure 12: Plaque load is not significantly altered in 3xTG mice after treatment, compared to PBS-treated controls. *This graph shows the results of a 6e10 staining in 3xTG mice. The x-axis shows the different groups: Male PBS (Blue) (n=6), Male Compound (Green) (n=6), Female PBS (Red) (n=13), Female Compound (Purple) (n=13). The y-axis shows the coverage of the staining in the subiculum of the ventral hippocampus in percentages (Coverage %). A) Quantification of extracellular 6e10 staining. B) Quantification of the intracellular 6e10 staining. Data represented as mean ± SEM. *p<0.05, **p<0.01.*

3.6 There is a significant weight difference between female 3xTG mice injected with the compound, compared to controls

During the treatment period, the mice were weighed every week. Figure 13 shows the results of these weights over 12 weeks of treatment. The graph shows the different groups over time. The x-axis shows the weeks, and the y-axis shows the weight in grams. The four groups are as follows: Male PBS (Blue) (n=12), Male Compound (Green) (n=13), Female PBS (Red) (n=15), Female Compound (Purple) (n=15). Overall, both female groups (Female PBS, Female Compound) have lost weight over time; however, it is visible that the PBS-treated mice lost less weight compared to the compound-treated mice. In the last 3 weeks of treatment, the weight difference was significant between the two groups, with a p-value of 0.0066. Within the male groups (Male Compound, Male PBS), there is no significant difference visible, with both groups having similar weights over time.

This data suggests that TNFR2 agonist treatment led to significant weight loss in female 3xTG mice compared to PBS controls, particularly in the final weeks of treatment, while male mice showed no significant changes in weight between groups.

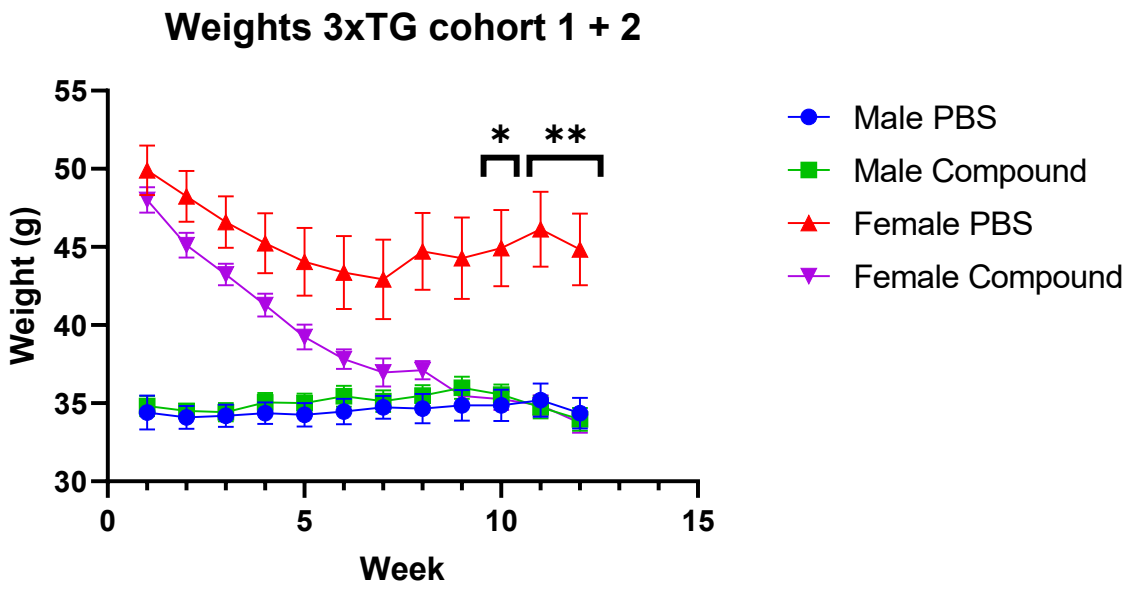

Figure 13: Female mice treated with the compound weigh significantly less than females treated with PBS. *The x-axis shows the weeks (Week), and the y-axis shows the weight in grams (Weight (g)). The four groups are as follows: Male PBS (Blue) (n=12), Male Compound (Green) (n=13), Female PBS (Red) (n=15), Female Compound (Purple) (n=15). * Data represented as mean ± SEM. *p<0.05, **p<0.01.*

4. Discussion

The goal of this research project was to assess the effects of a TNFR2 agonist on WT and 3xTG Alzheimer's mouse models. To do this, the following research question was formulated: “What is the effect of selective activation of TNFR2 in 3xTG and WT mouse models?” To address the main research question, two sub-questions were considered: (1) How does TNFR2 activation influence cognitive function? (2) What impact does it have on brain pathology in these mice?

Based on current insights, different outcomes were anticipated for the two models: In WT mice, no significant differences in behaviour or brain pathology are expected between treated and control groups, since these mice do not exhibit elevated neurodegeneration. In 3xTG mice, TNFR2 activation is expected to improve cognitive performance and reduce Aβ and tau pathology. This was studied by injecting the mice with a TNFR2 agonist twice a week and subjecting these mice to behavioural tests, including a Y-maze and MWM. After these tests were conducted, the mice were killed, and their brains were used for immunohistochemistry.

Following injection of the agonist in WT mice, no differences were observed in either the PBS-treated or agonist-treated groups, in terms of cognition or pathology/neuroinflammation. This finding is consistent with other studies that used WT mice as controls (Javonillo et al., 2022; Samaey et al., 2019). From these results, it can be concluded that the TNFR2 agonist does not negatively impact the wild-type mice, which supports our initial hypothesis that no change would be visible. However, the current study did not use female WT mice, which means that it was not possible to study the effect of the agonist in female mice.

In 3xTG mice, several results were seen. During the MWM, which tested the hippocampal memory of these mice, several differences were visible. During the training period of the MWM, it was observed that female mice treated with the agonist tended to perform better than those treated with PBS. This shows that the female mice treated with the agonist have fewer deficits in hippocampal memory compared to the PBS-treated controls. This decrease in escape latency is not seen within the males; in the males, both groups are the same. This is not in line with the hypothesis stated above, where it was hypothesised that the cognitive deficits would lessen.

Sex differences are also observed during the training period, as males performed significantly better than females. This has been shown in different studies, for example, in a study by Clinton et al. (2007) who studied the sexual dimorphisms in cognition and stress response in the 3xTG mice. They showed that at 4 months, the impairments are the same during the MWM; however, at higher ages, females perform worse than males. After 12 months, this difference is not visible anymore.

A possible explanation for these sex differences is the involvement of steroid hormones in cognition. Rosario et al. (2006) studied the effect of androgens on the development of AD in 3xTG mice. This study used gonadectomised (GDX) mice and sham-operated controls to investigate the effect of dihydrotestosterone (DHT) on pathology and cognition. It was shown that GDX mice had increased levels of Aβ and deficits in hippocampal function (Rosario et al., 2006). After DHT treatment, however, these cognitive deficits were attenuated. Another study by Hogervorst et al. (2005) investigated the effect of testosterone on cognition in elderly men and women, showing testosterone levels were lower in both males and females with AD compared to age-matched

individuals without AD. In addition to the role of testosterone, oestrogens are also known to affect cognition. During ageing, the levels of oestrogens decrease, and it was proposed by Yue et al. (2005) that this is a risk factor for the development of AD. In a postmortem analysis of female brains, it was found that those with AD showed greatly reduced oestrogen levels compared to age- and sex-matched controls. This study also examined the effect of oestrogen depletion in APP23 mice. This showed that oestrogen-depleted mice had more pathology compared to APP23 control mice (Yue et al., 2005).

This finding that DHT protects against the pathology and cognitive deficits of AD can explain the lack of cognitive deficits in males in the current study. Next to this, the increase in pathology when oestrogens are decreased can explain why the female mice have more pathology compared to males.

A limitation of the Morris water maze is that it is not possible to determine whether the deficits are due to AD-induced cognitive impairments or other variables such as stress, lack of motivation, or activity levels. Because the MWM is stressful, the study also examined the corticosterone levels of these mice and found that female 3xTG mice exhibit a heightened corticosterone response compared to males. Since these mice have a higher stress response, using a different test to assess their hippocampal memory might be more appropriate. An alternative to the MWM is the Barnes maze, which is less stressful, ensuring that observed results are attributable to cognitive deficits in AD rather than increased stress. It has been demonstrated by Stover et al. (2015) that 3xTG mice exhibit deficits in the Barnes maze, for example, indicating that it is a sensitive test for detecting cognitive impairments. This study found that 3xTG mice showed greater deficits compared to WT mice, with impairments observed in both male and female 3xTG mice (Stover et al., 2015).

The extracellular plaque load of female mice treated with the agonist was not decreased when compared to PBS-treated female mice. No extracellular plaques were observed in male mice. Intracellular Aβ was also stained, and showed a decrease in male mice treated with the agonist, compared to the PBS-treated males, and a small decrease in females treated with the agonist.

These finding are not in line with the hypothesis or with previous studies that evaluated the effect of a TNFR2 agonist. An example of such a study was done by Ortí-Casañ et al. (2022), which studied the effect of a TNFR2 agonist on a J20 mouse model. This study showed a decrease in plaques, contradicting our results. This difference in results could be explained by the difference between the 2 mouse models that were used. A study by Barber et al. (2024), which examined sex-specific disease trajectories in 3xTG mice, showed that plaque formation is both sex-dependent and distinct from other AD models. According to their findings, extracellular plaque accumulation begins around 15 months of age in female 3xTG mice, while male 3xTG mice do not develop extracellular plaques throughout their lifespan. Another study that looked at the pathology in 3xTG mice showed that at 9 months, there is still no soluble Aβ visible in both male and female 3xTG mice (Hirata-Fukae et al., 2008). This concentration of Aβ only starts to increase at 16 months in female mice (Hirata-Fukae et al., 2008). Next to extracellular Aβ plaques, there was also intracellular Aβ staining visible in these brain slices. This has been seen in other studies with 3xTG mice, an example being an experiment by Roda et al. (2020), who studied the effect of an anti-Aβ antibody fragment in older 3xTG mice, which is why the intracellular staining was also analysed in this study. Notably, plaques were not seen in the dorsal hippocampus, but were observed in the subiculum of the ventral hippocampus. This is consistent with observations made by Javonillo et

al. (2022) who characterised the pathology of the 3xTG mouse model, and also showed that there were no plaques visible in the dorsal hippocampus, and visualised the plaques in the subiculum.

Furthermore, Perez et al. (2010) demonstrated both sex differences and regional specificity in plaque formation: females began showing plaques at 8–9 months, while males developed them later, around 11–12 months. This may explain the absence of extracellular plaques in male mice in our study. , Perez et al. (2010) also reported intracellular Aβ in male 3xTG mice, aligning with our current findings. Additionally, they found that plaques primarily localise to the subiculum, further supporting our observations.

A possible explanation for the absence of plaques in male 3xTG mice, in contrast to the presence of plaques in females, is the difference in immunological profiles between the sexes. A study by Kapadia et al. (2018) which investigated the sex dependent differences in autoimmunity in 3xTG mice, found that there is more systemic autoimmunity in male 3xTG mice. This autoimmunity could interfere with the aggregation and development of plaques, causing no plaques to be formed in male 3xTG mice (Kapadia et al., 2018). The involvement of sex hormones could also explain these sex differences in pathology in 3xTG mice. A study by Carroll et al. (2010) studied the progression of Aβ pathology in male and female 3xTG mice and examined the effects of demasculinising or defeminising mice during early development. Their results showed a greater Aβ burden and more severe cognitive deficits in female mice. Moreover, demasculinised males exhibited increased Aβ accumulation, while defeminised females showed reduced pathology, displaying a more male-like pattern of Aβ development. These findings highlight the critical role of sex hormones in modulating AD-related pathology in the 3xTG mouse model. (Carroll et al., 2010).

No significant differences were observed in the Y maze in both males and females, which means that the agonist does not change the working memory in these mice. The total number of arm entries was very low, indicating that these mice were not very active. A study by Fertan et al. (2019) which used the Hebb-Williams maze to assess working memory, reported that female 3xTG mice exhibited motivational deficits and often did not consume the food reward (Fertan et al., 2019). This suggests that 3xTG mice may have reduced motivation to explore, which could limit the sensitivity of tasks like the Y-maze that rely on spontaneous exploration. As such, using an alternative behavioural test to assess working memory may be more informative. One such alternative is the novel object recognition (NOR) test, which evaluates memory by measuring the preference for exploring a novel object over a familiar one. A study by Chiquita et al. (2019) demonstrated that 3xTG mice exhibit cognitive impairments in this task compared to wild-type (WT) controls. Specifically, while WT mice showed a clear preference for the novel object, 3xTG mice explored both the familiar and novel objects equally, indicating a deficit in recognition memory.

Lastly, there was significant weight loss in females treated with the agonist. This has not been seen in other studies. The weight of the females in this experiment was, however, much higher compared to other studies that used 3xTG mice. In a study by Pairojana et al., the weight of the female 3xTG mice ranged from 20-40 grams, while in this study, the average weight ranged from 35-50 grams over 12 weeks. The weight loss of females could be explained by the increased stress of these females. A study by Nguyen et al. (2020), which studied the stress responsivity and social memory in 3xTG mice and showed that female mice have higher corticosterone levels than males.

A different study that assessed the stress response of 3xTG mice also showed increased corticosterone levels in female 3xTG mice, but not in males (Nguyen et al., 2020).

Additionally, sex differences were seen in body weight 3xTG mice, with females weighing more than the males at the start of the experiments, which is not in line with other studies Garvock-de Montbrun et al. (2019) which investigated the motor deficits in 3xTG mice, showed that there was a significant difference between male and female 3xTG mice; however, in this study, the males weighed more than the female mice. The study by Garvock-de Montbrun et al. (2019) also reported weight gain when the mice got older, this was, however, not the case in this study. This experiment showed a weight decrease in both the male and female mice.

Based on the results mentioned above, the following conclusions can be made: The TNFR2 agonist does not affect cognition in WT mice and does not change the neuroinflammation in these healthy mice.

In 3xTG mice, working memory is not affected by the TNFR2 agonist, but the agonist does tend to improve hippocampal memory in females treated with the agonist. Male mice have fewer cognitive deficits compared to female mice. Lastly, both intracellular and extracellular plaque load are not altered after treatment with the agonist in female mice, whereas intracellular Aβ staining is decreased in agonist-treated male mice.

These results suggest that female mice are more affected by AD-related pathology than male mice—a finding consistent with human data. In clinical populations, approximately two-thirds of Alzheimer's patients are female, highlighting the importance of considering sex as a biological variable in preclinical and clinical AD research (Burke et al., 2018).

A major strength of this study is that WT mice were used to test the agonist, as this shows that the agonist does not change or cause pathology in these healthy mice. Additionally, using a 3xTG mouse model makes it possible to study not only Aβ pathology but also tau pathology. This mimics the disease progression in humans better, which makes it more translatable for future human studies. Another strength is that the 3xTG mice were treated for 12 weeks, instead of the normal 6 weeks of injections, which visualises the long-term treatment effects better. Lastly, this study uses both sexes in the 3xTG mouse model, which makes it possible to study sex differences of this treatment option.

Some limitations of these experiments include the lack of females in the WT mouse model, making it impossible to study the effect of TNFR2 agonist treatment in healthy female mice. Additionally, the 3xTG mice were 10.5 months old, and very few plaques were seen at this age. Based on other studies mentioned before, it would be more effective to use older mice to increase pathology.

Future research should focus on repeating these experiments to replicate the results that were seen in this experiment. Next to this, it would be useful to use older mice to see the effects that happen in these mice. Using even older mice could be more representative of elderly people, as this group has the highest chance of getting AD. A study by Belfiore et al. (2019) studied the progression of disease pathology in female 3xTG mice, and studied this in mice that were 2-, 6-, 12- and 20-month-old, and showed that the pathology and cognition worsened over time.

Another promising avenue for future research is the inclusion of multiple time points for sacrifice and analysis. This longitudinal approach would allow researchers to track the progression of pathology and evaluate how the TNFR2 agonist affects the course of disease at different stages.

Furthermore, it may be beneficial to explore combination therapies involving both a TNFR2 agonist and a TNFR1 antagonist. Pegoretti et al. (2023) investigated this approach in an experimental autoimmune encephalomyelitis (EAE) mouse model, which mimics aspects of multiple sclerosis—a neurodegenerative disease also influenced by TNF signalling. This study found that stimulating TNFR2 and TNFR1 sequentially improved responses to treatment. The experiment also showed that the administration of both drugs was more effective than a single treatment with one of the two. As MS is a neurodegenerative disease and is also influenced by TNF signalling, this combined treatment could also help in AD. Next to this increased effectiveness of combining drugs, this combination could also allow for reduced dosages of each compound, potentially minimising side effects, while maintaining the therapeutic benefit.

Together, these findings contribute to a growing body of evidence supporting TNFR2 as a potential therapeutic target in Alzheimer's disease, while also emphasising the need for refined models and study designs that better reflect the heterogeneity of the human disease.

References

Barber, A. J., del Genio, C. L., Swain, A. B., Pizzi, E. M., Watson, S. C., Tapiavala, V. N., Zanazzi, G. J., & Gaur, A. B. (2024). Age, sex and Alzheimer's disease: a longitudinal study of 3xTg-AD mice reveals sex-specific disease trajectories and inflammatory responses mirrored in postmortem brains from Alzheimer's patients. *Alzheimer's Research and Therapy* , *16*(1), 1–24. https://doi.org/10.1186/S13195-024-01492-X/FIGURES/1

Belfiore, R., Rodin, A., Ferreira, E., Velazquez, R., Branca, C., Caccamo, A., & Oddo, S. (2019). Temporal and regional progression of Alzheimer's disease-like pathology in 3xTg-AD mice. *Aging Cell*, *18*(1). https://doi.org/10.1111/ACEL.12873,

Bode, D. C., Freeley, M., Nield, J., Palma, M., & Viles, J. H. (2019). Amyloid-β oligomers have a profound detergent-like effect on lipid membrane bilayers, imaged by atomic force and electron microscopy. *Journal of Biological Chemistry*, *294*(19), 7566–7572. https://doi.org/10.1074/JBC.AC118.007195/ATTACHMENT/4E677F3E-C34B-47E0-A27E-AFB1A2D45741/MMC1.ZIP

Bona, D. Di, Candore, G., Franceschi, C., Licastro, F., Colonna-Romano, G., Cammà, C., Lio, D., & Caruso, C. (2009). Systematic review by meta-analyses on the possible role of TNF-α polymorphisms in association with Alzheimer's disease. *Brain Research Reviews*, *61*(2), 60–68. https://doi.org/10.1016/j.brainresrev.2009.05.001

Breijyeh, Z., & Karaman, R. (2020). Comprehensive Review on Alzheimer's Disease: Causes and Treatment. *Molecules*, *25*(24), 5789. https://doi.org/10.3390/molecules25245789

Burke, S. L., Hu, T., Fava, N. M., Li, T., Rodriguez, M. J., Schuldiner, K. L., Burgess, A., & Laird, A. (2018). Sex differences in the development of mild cognitive impairment and probable Alzheimer's disease as predicted by the hippocampal volume or white matter hyperintensities. *Journal of Women & Aging*, *31*(2), 140. https://doi.org/10.1080/08952841.2018.1419476

Carroll, J. C., Rosario, E. R., Kreimer, S., Villamagna, A., Gentzschein, E., Stanczyk, F. Z., & Pike, C. J. (2010). Sex differences in β-amyloid accumulation in 3xTg-AD mice: Role of neonatal sex steroid hormone exposure. *Brain Research*, *1366*, 233–245. https://doi.org/10.1016/j.brainres.2010.10.009

Chabrier, M. A., Cheng, D., Castello, N. A., Green, K. N., & LaFerla, F. M. (2014). Synergistic effects of amyloid-beta and wild-type human tau on dendritic spine loss in a floxed double transgenic model of Alzheimer's disease. *Neurobiology of Disease*, *64*, 107–117. https://doi.org/10.1016/j.nbd.2014.01.007

Chiquita, S., Ribeiro, M., Castelhano, J., Oliveira, F., Sereno, J., Batista, M., Abrunhosa, A., Rodrigues-Neves, A. C., Carecho, R., Baptista, F., Gomes, C., Moreira, P. I., Ambrósio, A. F., & Castelo-Branco, M. (2019). A longitudinal multimodal in vivo molecular imaging study of the 3xTg-AD mouse model shows progressive early hippocampal and taurine loss. *Human Molecular Genetics*, *28*(13), 2174. https://doi.org/10.1093/HMG/DDZ045

Clinton, L. K., Billings, L. M., Green, K. N., Caccamo, A., Ngo, J., Oddo, S., McGaugh, J. L., & LaFerla, F. M. (2007). Age-dependent sexual dimorphisms in cognition and stress

response in the 3xTg-AD mice. *Neurobiology of Disease*, *28*(1), 76. https://doi.org/10.1016/J.NBD.2007.06.013

DiSabato, D. J., Quan, N., & Godbout, J. P. (2016). Neuroinflammation: the devil is in the details. *Journal of Neurochemistry*, *139*(S2), 136–153. https://doi.org/10.1111/jnc.13607

Dong, Y., Dekens, D. W., De Deyn, P. P., Naudé, P. J. W., & Eisel, U. L. M. (2015). Targeting of tumor necrosis factor alpha receptors as a therapeutic strategy for neurodegenerative disorders. In *Antibodies* (Vol. 4, Issue 4, pp. 369–408). MDPI. https://doi.org/10.3390/antib4040369

Dong, Y., Fischer, R., Naudé, P. J. W., Maier, O., Nyakas, C., Duffey, M., Van Der Zee, E. A., Dekens, D., Douwenga, W., Herrmann, A., Guenzi, E., Kontermann, R. E., Pfizenmaier, K., & Eisel, U. L. M. (2016). Essential protective role of tumor necrosis factor receptor 2 in neurodegeneration. *Proceedings of the National Academy of Sciences of the United States of America*, *113*(43), 12304–12309. https://doi.org/10.1073/pnas.1605195113

Fertan, E., Wong, A. A., Vienneau, N. A., & Brown, R. E. (2019). Age and sex differences in motivation and spatial working memory in 3xTg-AD mice in the Hebb–Williams maze. *Behavioural Brain Research*, *370*. https://doi.org/10.1016/j.bbr.2019.111937

Fillit, H., Ding, W., Buee, L., Kalman, J., Altstiel, L., Lawlor, B., & Wolf-Klein, G. (1991). Elevated circulating tumor necrosis factor levels in Alzheimer's disease. *Neuroscience Letters*, *129*(2), 318–320. https://doi.org/10.1016/0304-3940(91)90490-K

Fischer, R., Kontermann, R. E., & Maier, O. (2015). Targeting sTNF/TNFR1 signaling as a new therapeutic strategy. In *Antibodies* (Vol. 4, Issue 1, pp. 48–70). MDPI. https://doi.org/10.3390/antib4010048

Gamblin, T. C., Chen, F., Zambrano, A., Abraha, A., Lagalwar, S., Guillozet, A. L., Lu, M., Fu, Y., Garcia-Sierra, F., LaPointe, N., Miller, R., Berry, R. W., Binder, L. I., & Cryns, V. L. (2003). Caspase cleavage of tau: Linking amyloid and neurofibrillary tangles in Alzheimer's disease. *Proceedings of the National Academy of Sciences*, *100*(17), 10032–10037. https://doi.org/10.1073/pnas.1630428100

Garvock-de Montbrun, T., Fertan, E., Stover, K., & Brown, R. E. (2019). Motor deficits in 16-month-old male and female 3xTg-AD mice. *Behavioural Brain Research*, *356*, 305–313. https://doi.org/10.1016/J.BBR.2018.09.006

He, Z., Guo, J. L., McBride, J. D., Narasimhan, S., Kim, H., Changolkar, L., Zhang, B., Gathagan, R. J., Yue, C., Dengler, C., Stieber, A., Nitla, M., Coulter, D. A., Abel, T., Brunden, K. R., Trojanowski, J. Q., & Lee, V. M.-Y. (2018). Amyloid-β plaques enhance Alzheimer's brain tau-seeded pathologies by facilitating neuritic plaque tau aggregation. *Nature Medicine*, *24*(1), 29–38. https://doi.org/10.1038/nm.4443

Hickman, S. E., Allison, E. K., & El Khoury, J. (2008). Microglial Dysfunction and Defective β-Amyloid Clearance Pathways in Aging Alzheimer's Disease Mice. *The Journal of Neuroscience*, *28*(33), 8354. https://doi.org/10.1523/JNEUROSCI.0616-08.2008

Hirata-Fukae, C., Li, H. F., Hoe, H. S., Gray, A. J., Minami, S. S., Hamada, K., Niikura, T., Hua, F., Tsukagoshi-Nagai, H., Horikoshi-Sakuraba, Y., Mughal, M., Rebeck, G. W., LaFerla,

F. M., Mattson, M. P., Iwata, N., Saido, T. C., Klein, W. L., Duff, K. E., Aisen, P. S., & Matsuoka, Y. (2008). Females exhibit more extensive amyloid, but not tau, pathology in an Alzheimer transgenic model. *Brain Research*, *1216*, 92–103. https://doi.org/10.1016/j.brainres.2008.03.079

Hogervorst, E., Bandelow, S., & Moffat, S. D. (2005). Increasing testosterone levels and effects on cognitive functions in elderly men and women: A review. *Current Drug Targets: CNS and Neurological Disorders*, *4*(5), 531–540. https://doi.org/10.2174/156800705774322049,

Idriss, H. T., & Naismith, J. H. (2000). TNF-alpha and the TNF receptor superfamily: Structure-function relationship(s). *Microscopy Research and Technique*, *50*(3), 184–195. https://doi.org/10.1002/1097-0029(20000801)50:3<184::AID-JEMT2>3.0.CO;2-H

Javonillo, D. I., Tran, K. M., Phan, J., Hingco, E., Kramár, E. A., da Cunha, C., Forner, S., Kawauchi, S., Milinkeviciute, G., Gomez-Arboledas, A., Neumann, J., Banh, C. E., Huynh, M., Matheos, D. P., Rezaie, N., Alcantara, J. A., Mortazavi, A., Wood, M. A., Tenner, A. J., … LaFerla, F. M. (2022). Systematic Phenotyping and Characterization of the 3xTg-AD Mouse Model of Alzheimer's Disease. *Frontiers in Neuroscience*, *15*, 785276. https://doi.org/10.3389/FNINS.2021.785276/FULL

Kapadia, M., Mian, M. F., Michalski, B., Azam, A. B., Ma, D., Salwierz, P., Christopher, A., Rosa, E., Zovkic, I. B., Forsythe, P., Fahnestock, M., & Sakic, B. (2018). Sex-Dependent Differences in Spontaneous Autoimmunity in Adult 3xTg-AD Mice. *Journal of Alzheimer's Disease*, *63*(3), 1191–1205. https://doi.org/10.3233/JAD-170779,

Kitazawa, M., Oddo, S., Yamasaki, T. R., Green, K. N., & LaFerla, F. M. (2005). Lipopolysaccharide-Induced Inflammation Exacerbates Tau Pathology by a Cyclin-Dependent Kinase 5-Mediated Pathway in a Transgenic Model of Alzheimer's Disease. *The Journal of Neuroscience*, *25*(39), 8843–8853. https://doi.org/10.1523/JNEUROSCI.2868-05.2005

Koenigsknecht-Talboo, J., & Landreth, G. E. (2005). Microglial Phagocytosis Induced by Fibrillar β-Amyloid and IgGs Are Differentially Regulated by Proinflammatory Cytokines. *The Journal of Neuroscience*, *25*(36), 8240–8249. https://doi.org/10.1523/JNEUROSCI.1808-05.2005

Kukull, W. A., Higdon, R., Bowen, J. D., McCormick, W. C., Teri, L., Schellenberg, G. D., van Belle, G., Jolley, L., & Larson, E. B. (2002). Dementia and Alzheimer Disease Incidence. *Archives of Neurology*, *59*(11), 1737. https://doi.org/10.1001/archneur.59.11.1737

Lee, J. W., Lee, Y. K., Yuk, D. Y., Choi, D. Y., Ban, S. B., Oh, K. W., & Hong, J. T. (2008). Neuro-inflammation induced by lipopolysaccharide causes cognitive impairment through enhancement of beta-amyloid generation. *Journal of Neuroinflammation*, *5*(1), 37. https://doi.org/10.1186/1742-2094-5-37

Li, J., Zhang, Z., Wu, X., Zhou, J., Meng, D., & Zhu, P. (2021). Risk of Adverse Events After Anti-TNF Treatment for Inflammatory Rheumatological Disease. A Meta-Analysis. *Frontiers in Pharmacology*, *12*. https://doi.org/10.3389/fphar.2021.746396

Nguyen, E. T., Selmanovic, D., Maltry, M., Morano, R., Franco-Villanueva, A., Estrada, C. M., & Solomon, M. B. (2020). Endocrine stress responsivity and social memory in 3xTg-AD

female and male mice: A tale of two experiments. *Hormones and Behavior*, *126*. https://doi.org/10.1016/j.yhbeh.2020.104852

Ortí-Casañ, N., Boerema, A. S., Köpke, K., Ebskamp, A., Keijser, J., Zhang, Y., Chen, T., Dolga, A. M., Broersen, K., Fischer, R., Pfizenmaier, K., Kontermann, R. E., & Eisel, U. L. M. (2023). The TNFR1 antagonist Atrosimab reduces neuronal loss, glial activation and memory deficits in an acute mouse model of neurodegeneration. *Scientific Reports*, *13*(1). https://doi.org/10.1038/s41598-023-36846-2

Ortí-Casañ, N., Wajant, H., Kuiperij, H. B., Hooijsma, A., Tromp, L., Poortman, I. L., Tadema, N., De Lange, J. H. E., Verbeek, M. M., De Deyn, P. P., Naud, P. J. W., & Eisel, U. L. M. (2023). Activation of TNF Receptor 2 Improves Synaptic Plasticity and Enhances Amyloid-β Clearance in an Alzheimer's Disease Mouse Model with Humanized TNF Receptor 2. *Journal of Alzheimer's Disease*, *94*(3), 977–991. https://doi.org/10.3233/JAD-221230

Ortí-Casañ, N., Zuhorn, I. S., W Naud, P. J., De Deyn, P. P., M van Schaik, P. E., Wajant, H., & M Eisel, U. L. (2022). *A TNF receptor 2 agonist ameliorates neuropathology and improves cognition in an Alzheimer's disease mouse model*. https://doi.org/10.1073/pnas

Ott, A., Breteler, M. M. B., van Harskamp, F., Claus, J. J., van der Cammen, T. J. M., Grobbee, D. E., & Hofman, A. (1995). Prevalence of Alzheimer's disease and vascular dementia: association with education. The Rotterdam study. *BMJ*, *310*(6985), 970–973. https://doi.org/10.1136/bmj.310.6985.970

Pairojana, T., Phasuk, S., Suresh, P., Huang, S. P., Pakaprot, N., Chompoopong, S., Hsieh, T. C., & Liu, I. Y. (2021). Age and gender differences for the behavioral phenotypes of 3xTg alzheimer's disease mice. *Brain Research*, *1762*, 147437. https://doi.org/10.1016/J.BRAINRES.2021.147437

Pegoretti, V., Bauer, J., Fischer, R., Paro, I., Douwenga, W., Kontermann, R. E., Pfizenmaier, K., Houben, E., Broux, B., Hellings, N., Baron, W., Laman, J. D., & Eisel, U. L. M. (2023). Sequential treatment with a TNFR2 agonist and a TNFR1 antagonist improves outcomes in a humanized mouse model for MS. *Journal of Neuroinflammation*, *20*(1), 106. https://doi.org/10.1186/s12974-023-02785-y

Perez, S. E., He, B., Muhammad, N., Oh, K. J., Fahnestock, M., Ikonomovic, M. D., & Mufson, E. J. (2010). Cholinotrophic basal forebrain system alterations in 3xTg-AD transgenic mice. *Neurobiology of Disease*, *41*(2), 338. https://doi.org/10.1016/J.NBD.2010.10.002

Richter, F., Seifert, O., Herrmann, A., Pfizenmaier, K., & Kontermann, R. E. (2019). Improved monovalent TNF receptor 1-selective inhibitor with novel heterodimerizing Fc. *MAbs*, *11*(4), 653–665. https://doi.org/10.1080/19420862.2019.1596512

Roda, A. R., Montoliu-Gaya, L., Serra-Mir, G., & Villegas, S. (2020). Both Amyloid-β Peptide and Tau Protein Are Affected by an Anti-Amyloid-β Antibody Fragment in Elderly 3xTg-AD Mice. *International Journal of Molecular Sciences 2020, Vol. 21, Page 6630*, *21*(18), 6630. https://doi.org/10.3390/IJMS21186630

Rosario, E. R., Carroll, J. C., Oddo, S., LaFerla, F. M., & Pike, C. J. (2006). Androgens Regulate the Development of Neuropathology in a Triple Transgenic Mouse Model of

Alzheimer's Disease. *The Journal of Neuroscience*, *26*(51), 13384. https://doi.org/10.1523/JNEUROSCI.2514-06.2006

Samaey, C., Schreurs, A., Stroobants, S., & Balschun, D. (2019). Early Cognitive and Behavioral Deficits in Mouse Models for Tauopathy and Alzheimer's Disease. *Frontiers in Aging Neuroscience*, *11*, 335. https://doi.org/10.3389/FNAGI.2019.00335/FULL

Shankar, G. M., Li, S., Mehta, T. H., Garcia-Munoz, A., Shepardson, N. E., Smith, I., Brett, F. M., Farrell, M. A., Rowan, M. J., Lemere, C. A., Regan, C. M., Walsh, D. M., Sabatini, B. L., & Selkoe, D. J. (2008). Amyloid-β protein dimers isolated directly from Alzheimer's brains impair synaptic plasticity and memory. *Nature Medicine*, *14*(8), 837–842. https://doi.org/10.1038/nm1782

Sheppard, O., & Coleman, M. (2020). Alzheimer's Disease: Etiology, Neuropathology and Pathogenesis. In *Alzheimer's Disease: Drug Discovery* (pp. 1–22). Exon Publications. https://doi.org/10.36255/exonpublications.alzheimersdisease.2020.ch1

Singh, J. A., Wells, G. A., Christensen, R., Tanjong Ghogomu, E., Maxwell, L. J., MacDonald, J. K., Filippini, G., Skoetz, N., Francis, D. K., Lopes, L. C., Guyatt, G. H., Schmitt, J., La Mantia, L., Weberschock, T., Roos, J. F., Siebert, H., Hershan, S., Cameron, C., Lunn, M. P., … Buchbinder, R. (2011). Adverse effects of biologics: a network meta-analysis and Cochrane overview. *Cochrane Database of Systematic Reviews*, *2016*(4). https://doi.org/10.1002/14651858.CD008794.pub2

Steverson, M. (2024, October 1). *Ageing and health*. World Health Organisation (WHO).

Stover, K. R., Campbell, M. A., Van Winssen, C. M., & Brown, R. E. (2015). Early detection of cognitive deficits in the 3xTg-AD mouse model of Alzheimer's disease. *Behavioural Brain Research*, *289*, 29–38. https://doi.org/10.1016/J.BBR.2015.04.012

Tansey, M., & McAlpine. (2008). Neuroinflammation and tumor necrosis factor signaling in the pathophysiology of Alzheimer's disease. *Journal of Inflammation Research*, 29. https://doi.org/10.2147/JIR.S4397

Tanzi, R. E., & Bertram, L. (2005). Twenty Years of the Alzheimer's Disease Amyloid Hypothesis: A Genetic Perspective. *Cell*, *120*(4), 545–555. https://doi.org/10.1016/j.cell.2005.02.008

Torres-Acosta, N., O'Keefe, J. H., O'Keefe, E. L., Isaacson, R., & Small, G. (2020). Therapeutic Potential of TNF-α Inhibition for Alzheimer's Disease Prevention. *Journal of Alzheimer's Disease*, *78*(2), 619–626. https://doi.org/10.3233/JAD-200711

Walter, S., Letiembre, M., Liu, Y., Heine, H., Penke, B., Hao, W., Bode, B., Manietta, N., Walter, J., Schulz-Schüffer, W., & Fassbender, K. (2007). Role of the Toll-Like Receptor 4 in Neuroinflammation in Alzheimer's Disease. *Cellular Physiology and Biochemistry*, *20*(6), 947–956. https://doi.org/10.1159/000110455

Wyss-Coray, T., Loike, J. D., Brionne, T. C., Lu, E., Anankov, R., Yan, F., Silverstein, S. C., & Husemann, J. (2003). Adult mouse astrocytes degrade amyloid-β in vitro and in situ. *Nature Medicine*, *9*(4), 453–457. https://doi.org/10.1038/NM838,

Yiannopoulou, K. G., & Papageorgiou, S. G. (2020). Current and Future Treatments in Alzheimer Disease: An Update. *Journal of Central Nervous System Disease*, *12*, 117957352090739. https://doi.org/10.1177/1179573520907397

Yue, X., Lu, M., Lancaster, T., Cao, P., Honda, S. I., Staufenbiel, M., Harada, N., Zhong, Z., Shen, Y., & Li, R. (2005). Brain estrogen deficiency accelerates Aβ plaque formation in an Alzheimer's disease animal model. *Proceedings of the National Academy of Sciences of the United States of America*, *102*(52), 19198. https://doi.org/10.1073/PNAS.0505203102

Zhang, W., Xiao, D., Mao, Q., & Xia, H. (2023). Role of neuroinflammation in neurodegeneration development. *Signal Transduction and Targeted Therapy*, *8*(1), 267. https://doi.org/10.1038/s41392-023-01486-5

AI statement

ChatGPT was used to do spelling checks and to rewrite sentences that were not grammatically correct.

Appendix

A1: Antibodies used to stain the blood extracellularly. The table shows each antibody that was used, what dilution it was used in, what fluorochrome the marker was linked to and lastly both the product number and company of the antibody.

Fluorochrome	Marker	Dilution	Product number	Company
BV421	TIGIT	1:100	#565270	BD biosciences
BV510	CD4	1:200	#100559	Biolegend
BV605	Lag3	1:100	#745214	BD biosciences
BV711	CD25	1:100	#740714	BD biosciences
BV786	CD62L	1:200	#104440	Biolegend
FITC	CD44	1:100	#553133	BD biosciences
PE	TNFR2	1:100	#113406	Biolegend
PerCPeF710	CD8	1:100	#46-0081-82	Invitrogen
APC	TNFR1	1:100	#113006	Biolegend
APCeF780	Live/Dead Zombie NIR	1:1000	#423106	Biolegend

A2: Region of interests of the CD68/GFAP staining in WT brains. The figure shows a dorsal hippocampus slice, in which the CA1 (1), CA3 (2), Dentate Gyrus (3), corpus callosum (4), and cortex (5) was selected on the left and right side of the brain.

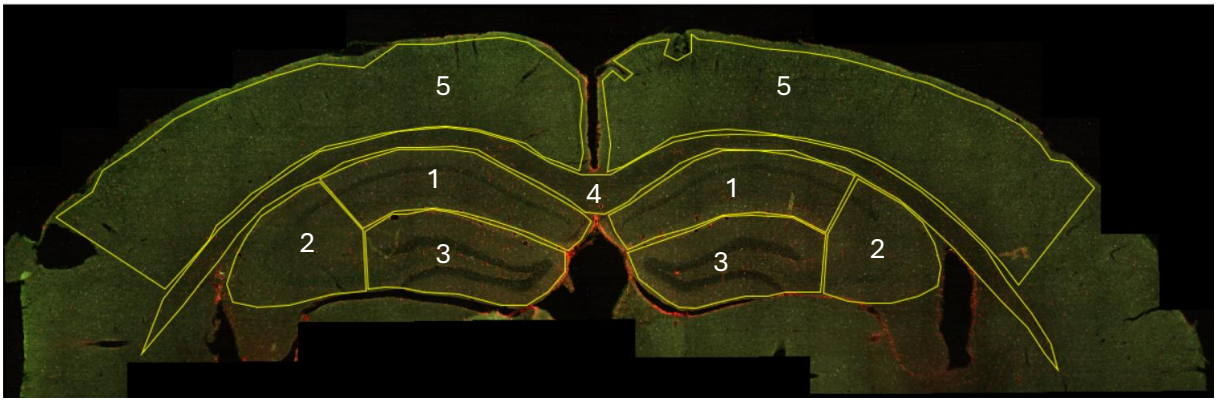

A3: Region of interest of the 6e10 staining in 3xTG brains. The figure shows a ventral hippocampus slice, in which the subiculum is selected as region of interest in the left and right side of the brain.

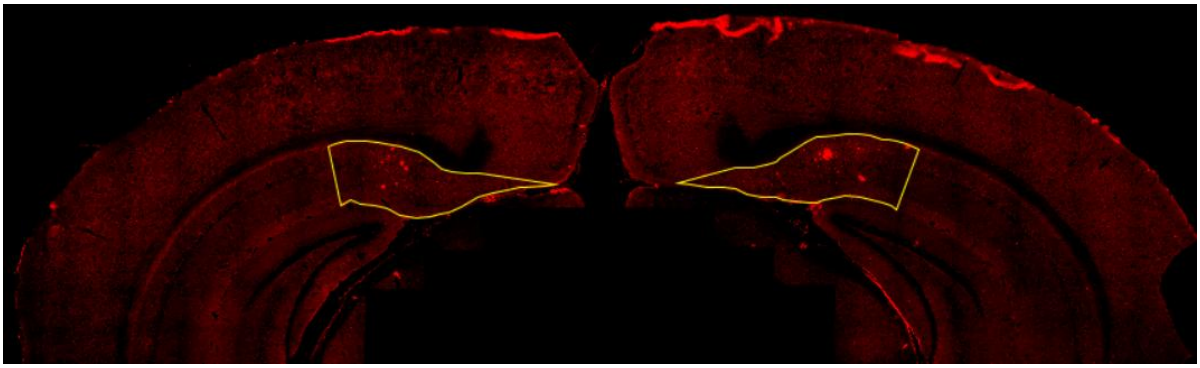

A4: Immunohistochemistry results of WT mice. The figure shows the results of both the GFAP and CD68 staining in WT mice. The left figures in red show the GFAP results of a PBS and Compound mouse, the middle figures in green show the CD68 results, and the right figures show an overlay of both stainings.